RSC Advances

PAPER

View Article Online
View Journal | View Issue

Cite this: *RSC Adv.*, 2025, **15**, 19456

Green facile fabrication of halogen-free flame-retardant ABS with high mechanical performance†

Ping Meng,[ab] Hong-Ren Xiao,[b] Feng Zhang,[ab] Rui-Sheng Jia,[c] Longxiang Zhu*[ab] and Zhu-Bao Shao *[ab]

Received 26th February 2025
Accepted 25th May 2025

DOI: 10.1039/d5ra01392e

rsc.li/rsc-advances

The development of halogen-free flame-retardant acrylonitrile-butadiene-styrene (ABS) with both high fire safety and excellent mechanical properties remains a significant challenge. Herein, cerium chemical hybrid ammonium polyphosphate (Ce@APP) was synthesized through an ion-exchange reaction in a water–ethanol solvent, and halogen-free intumescent flame-retardant ABS composites (denoted as ABS6) were fabricated by incorporating a phosphamide derivative (DP). Different from the APP/DP system, the excellent synergistic effects of Ce@APP/DP, including strong catalytic cross-linking carbonization, gaseous dilution and capture mechanism at high temperatures (especially above 570 °C), endowed the ABS composites with excellent fire safety. ABS6 achieved a limited oxygen index (LOI) of 28.6% and satisfied the UL-94 V0 rating. Furthermore, compared with those of pristine ABS, the peak heat release rate (pHRR) and peak smoke production rate (pSPR) of ABS6 were reduced by 76.6% and 65.9%, respectively. Notably, the good interfacial compatibility between the Ce@APP/DP system and the ABS matrix mitigated the deterioration of mechanical properties. The tensile and flexural strengths of ABS6 remained nearly the same, while its impact strength remained at 4.02 kJ m^{-2}. This green, facile fabrication offers a promising approach for developing halogen-free flame-retardant ABS.

1 Introduction

ABS is a rubber-toughened thermoplastic engineering plastic; owing to its excellent toughness, low-temperature impact resistance, high gloss, and ease of processing,[1,2] it has been widely utilized in the electronics and electrical industries.[3–5] However, ABS exhibits high flammability with rapid flame spread and significant smoke generation, thereby posing considerable fire hazards to life and property.[6] To address these challenges, it is essential to enhance the fire safety of ABS. Currently, commercial flame-retardant ABS composites primarily rely on halogen flame retardants through gas-phase mechanisms.[7,8] However, considering environmental and health concerns, the application of halogen flame retardants have been limited. Consequently, research on halogen-free flame-retardant systems for ABS has emerged as a critical focus.

The development of halogen-free flame-retardant ABS has exhibited slow progress owing to these challenges.[9,10] ABS consists of polystyrene, polybutadiene, and polyacrylonitrile, which are inherently flammable and difficult to carbonize.[11–13] Furthermore, the distinct combustion mechanisms of these components complicate the overall combustion behavior of ABS. Unlike other materials, the molecular components of ABS lack oxygen-containing groups; thus, the ABS composite does not readily undergo dehydration and carbonization with acid sources to form stable char layers.[14–16] Moreover, massive amounts of smoke are produced during ABS combustion.[17,18] Some traditional halogen-free flame retardants enable the flame retardancy of ABS composites, but this is often accompanied by the generation of more toxic and harmful gases.[19] Thus, the development of halogen-free flame-retardant ABS composites remains a significant challenge.

Currently, halogen-free flame-retardant treatments for polymer materials are primarily categorized into two approaches: intrinsic flame retardants and additive flame retardants.[20,21] For ABS, intrinsic flame retardants could favor the mechanical properties. However, owing to the particularity of ABS compositions and structures, the synthesis process for intrinsic flame-retardant ABS composites remains intricate and has progressed slowly. Therefore, additive flame retardants dominate ABS flame-retardant strategies due to its simple preparation and easy processing. Currently, the commonly additive flame retardants mainly contain metal

[a]College of Chemistry and Chemical Engineering, Qingdao University, Ningxia Road, 308, Qingdao 266071, China. E-mail: lxzhu@qdu.edu.cn; zhu871227@163.com
[b]Institute of Functional Textiles and Advanced Materials, National Engineering Research Center for Advanced Fire-Safety Materials D & A (Shandong), Qingdao Key Laboratory of Flame-Retardant Textile Materials, College of Textiles and Clothing, Qingdao University, Ningxia Road, 308, Qingdao 266071, China
[c]Jilin Baien Plastic Technology Co., Ltd, Ruipeng Road 1592, Changchun 130000, China

† Electronic supplementary information (ESI) available. See DOI: https://doi.org/10.1039/d5ra01392e

hydroxides, silicon-, nano-, phosphorus-, and intumescent flame retardant systems.[22,23] Although metal hydroxides exhibit good heat reduction and smoke suppression, their flame-retardant efficiency is low. High loading often seriously deteriorates the mechanical properties of ABS.[24–26] Metal hypophosphites combine both condensed-phase and gas-phase mechanisms.[27] However, its weak interfacial interaction with ABS makes it prone to forming stress concentration points under external forces, which compromises the toughened structure between the ABS phases. Intumescent flame retardants, integrating acid sources, gas sources, and carbon sources, can promote the formation of porous intumescent carbon layers when exposed to heat or flames,[28] which can insulate the material from heat and oxygen, and provide effective flame retardancy. APP/oligoamides and monospirocyclic phosphonates have achieved promising flame retardance.[29] Therefore, achieving an optimal balance between flame retardancy and the mechanical performance of ABS composites has attracted growing attention.

It has been reported that certain metals and their compounds exhibit excellent catalytic carbonization and smoke suppression properties,[30,31] which can effectively promote the rapid carbonization of polymer matrices and/or carbon-forming agents during heating and/or combustion. Additionally, catalytic carbonization facilitates the conversion of pyrolysis components into condensed-phase carbon layers, thereby reducing smoke release and enhancing fire safety. Inspired by this, cerium-modified ammonium polyphosphate (Ce@APP) was designed and prepared. The ABS/Ce@APP/DP composites were developed by incorporating Ce@APP and the phosphorus-containing gas-phase flame retardant (DP). The thermal performance and flame retardancy of the ABS/Ce@APP/DP composites were investigated. The flame-retardant mechanism combining the condensed and gas phases was investigated in detail. Furthermore, the excellent interfacial compatibility between the Ce@APP/DP system and the ABS matrix mitigated damage to the interphase toughening structures of ABS.

2. Experimental section

2.1 Materials and characterization

The materials and detailed characterizations are provided in the ESI.†

2.2 Preparation of Ce@APP

The synthetic route of Ce@APP is presented in Fig. 1. 8 g cerium chloride was poured into a mixed solvent of 300 mL ethanol and 20 mL water and stirred for 30 min until dissolved. Then, 20 g APP was added and stirred for 12 h at room temperature. Next, the white solid product was filtered, washed five times with ethanol, and dried in an oven at 80 °C. The yield of Ce@APP was 67%.

2.3 Preparation of DP

The synthesis of DP was performed according to our previous work.[32]

2.4 Preparation of flame-retardant ABS composites

ABS composites were prepared using an internal mixer equipped with three heating zones, each maintained at a temperature of 220 °C and a rotor speed of 100 rpm. The desired amounts of flame retardants were premixed with ABS and then introduced into the internal mixer. The formulations of the prepared samples are summarized in Table 1. Subsequently, the ABS composite samples were molded under a pressure of 10 MPa for 10 min at 200 °C.

Table 1 Formulations of ABS composites

Sample	ABS (g)	APP (g)	Ce@APP (g)	DP (g)
ABS1	50.00	—	—	—
ABS2	35.00	15.00	—	—
ABS3	35.00	11.25	—	3.750
ABS4	37.50	—	9.375	3.125
ABS5	36.00	—	10.50	3.500
ABS6	35.00	—	11.25	3.750

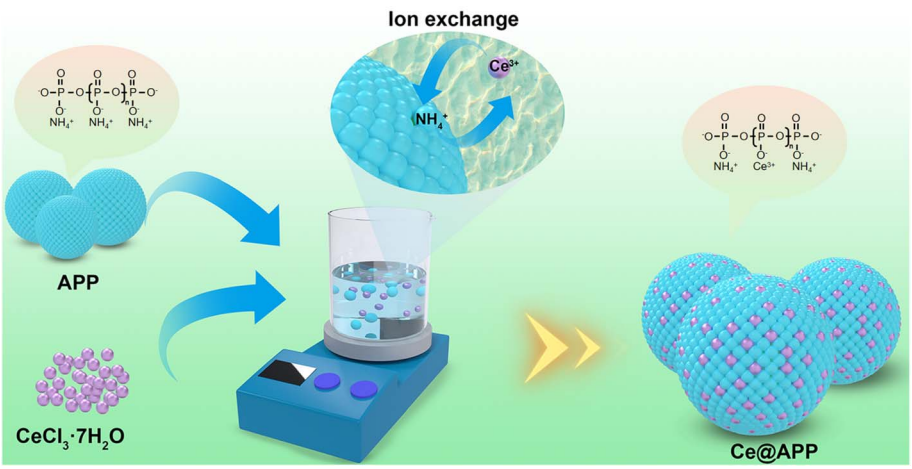

Fig. 1 Synthetic route of Ce@APP.

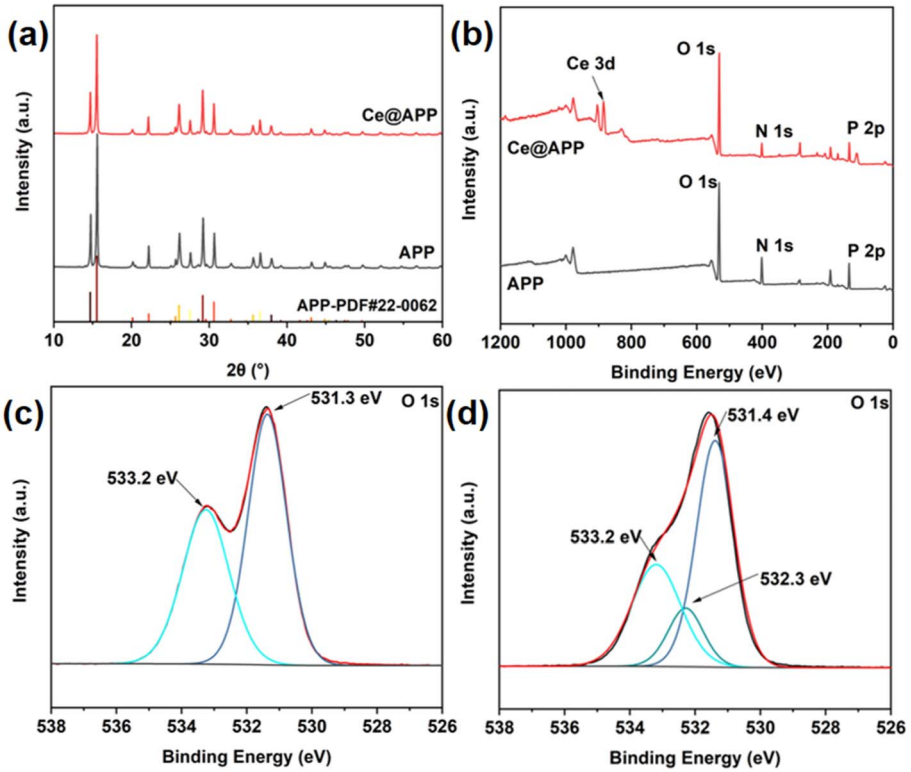

Fig. 2 XRD patterns of APP and Ce@APP (a). XPS survey spectra of APP and Ce@APP (b). The corresponding XPS spectra of O 1s of APP (c) and Ce@APP (d).

3. Results and discussion

3.1 Characterization of Ce@APP

The X-ray diffraction (XRD) patterns for Ce@APP are presented in Fig. 2a. The diffraction peaks of Ce@APP were similar to those of APP, and no other new peaks were observed. This indicates that the modification did not affect the crystal structure of APP. X-ray photoelectron spectroscopy (XPS) was carried out to analyze the chemical states of the elements in Ce@APP. As shown in Fig. 2b, compared to APP, besides the characteristic peaks of N, O and P elements, Ce@APP exhibited an obvious characteristic peak in the range of 880–920 eV, corresponding to the cerium element, which confirms the presence of cerium in Ce@APP. The intensity of the cerium characteristic peak is similar to that of the phosphorus and nitrogen characteristic peaks. In contrast, the intensity of the nitrogen characteristic peak in APP is slightly higher than that in Ce@APP, further confirming that cerium ions replaced a significant number of ammonium ions during the ion exchange process. Additionally, the O 1s spectra for APP and Ce@APP were deconvoluted, as shown in Fig. 2c and d. For Ce@APP, besides the characteristic signal peaks of –O–, P═O, and $-O^{-}NH_4^{+}$ of APP at binding energies of 531.3 eV and 533.2 eV,[33] a new signal peak attributed to $-O^{-}Ce^{3+}$ was identified at 532.3 eV. These results demonstrated that Ce^{3+} was successfully incorporated into APP.

The microstructures of Ce@APP are presented in Fig. 3. Compared to the unmodified APP (Fig. 3a and a′), the surface of Ce@APP displayed a relatively rough surface (Fig. 3b and b′), and the Ce element was uniformly dispersed on the surface of Ce@APP, as depicted in Fig. 3c. Furthermore, the Ce and P contents in Ce@APP were 1.2 wt% and 32.7 wt% by the inductively coupled plasma optical emission spectroscopy (ICP-OES) test, respectively. These findings further proved that Ce@APP was successfully synthesized.

3.2 Thermal analysis

The thermal stability of APP and Ce@APP is presented in Fig. 4 and Table S1.† Both APP and Ce@APP exhibited similar thermal decomposition behavior, which is mainly divided into two main thermal-degradation stages. During 250–470 °C, the mass loss was attributed to the decomposition of unstable structures in APP, leading to the release of ammonia, water, *etc.*[34] The second stage at 470–750 °C involved the thermal condensation of the polyphosphoric acid structures in APP, resulting in the production of phosphoric acid, polyphosphoric acid, and pyrophosphoric acid.[35] Although Ce@APP possessed the same thermal decomposition trend as APP before 570 °C, significant differences emerged beyond this temperature. Specifically, Ce@APP demonstrated an earlier onset of thermal degradation after 570 °C, but with a notably reduced thermal weight loss rate. Thus, the residual weight at 750 °C for Ce@APP (33.4 wt%) was higher than that of pure APP (31.6 wt%). These phenomena indicated that the presence of the cerium element in Ce@APP accelerated the thermal decomposition and polycondensation of APP after 570 °C, resulting in the formation of phosphoric acid derivatives that exhibited better thermal stability. These derivatives could promote cross-linking and carbonization

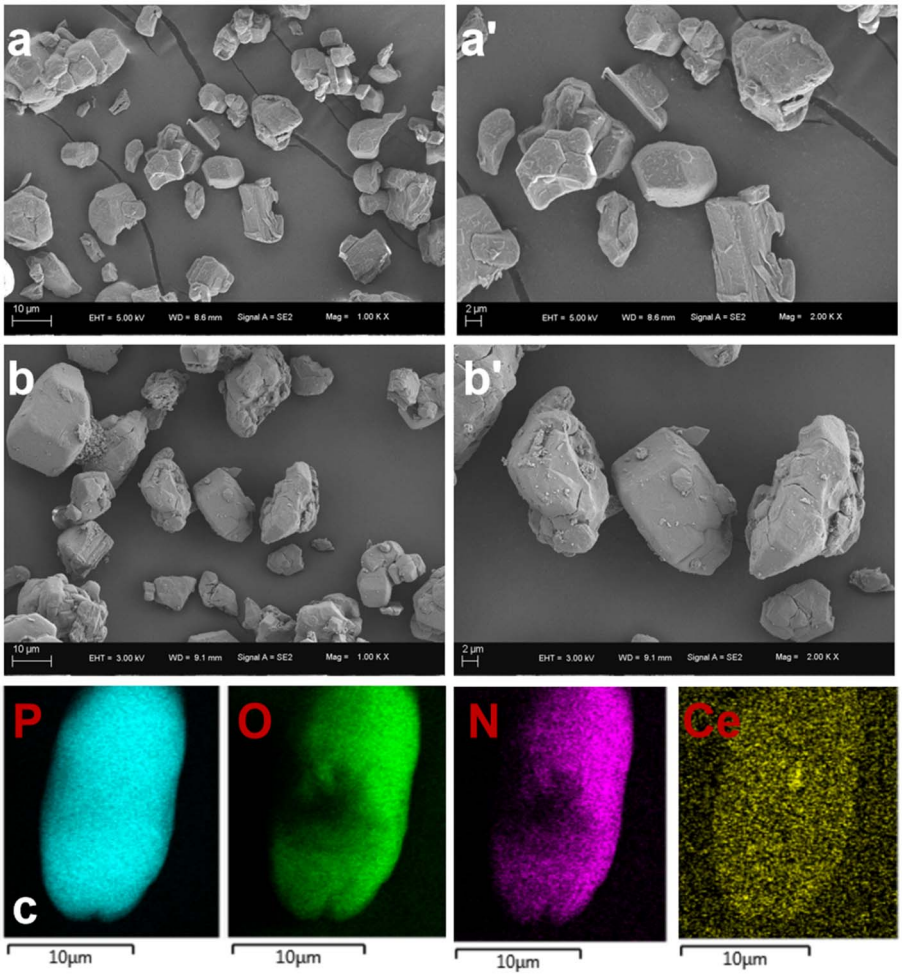

Fig. 3 Morphology of neat APP (a and a′) and Ce@APP (b and b′). The corresponding elemental mappings of Ce@APP (c).

reactions with carbon-forming groups, thereby generating a high-temperature-resistant carbon layer with a robust physical barrier effect.

As illustrated in Fig. 4c and d, pure ABS in a nitrogen atmosphere underwent a single thermal decomposition stage within the temperature range of 370–500 °C, with almost no residuals left at 750 °C. With the addition of APP, the thermal decomposition behavior of ABS2 before 450 °C was nearly similar to that of ABS1. Here, the initial decomposition temperature of ABS2 slightly decreased due to the early decomposition of APP. However, beyond 450 °C, the thermal degradation rate of ABS2 significantly decreased, and the residuals at 750 °C increased to 10.3 wt%. This increase was attributed to the high thermal stability of APP, which generated phosphorus-containing derivatives that promoted the carbonization of ABS. When APP/DP and Ce@APP/DP were introduced into ABS, the initial decomposition temperatures of ABS3 and ABS6 decreased to 328.6 °C and 330.2 °C, respectively. The early decomposition of APP/DP and Ce@APP/DP facilitated the generation of nonflammable gases and/or an expandable carbon layer, thereby enhancing the fire safety of ABS composites. In the range of 570–750 °C, the residual contents of ABS3 and ABS2 remained consistent at 10.3 wt% because DP degraded and produced substantial quantities of gaseous phosphorus derivatives during thermal decomposition.[32] This observation highlights the difficulty of achieving a synergistic condensed-phase flame-retardant effect between APP and DP at high temperatures. Furthermore, the thermal decomposition trends of ABS3 and ABS6 are identical before 570 °C, implying that the presence of the cerium element does not affect the decomposition process of the ABS/APP/DP system within this temperature range. However, beyond 570 °C, ABS6 reaches thermal stability equilibrium earlier than ABS3, with a residual mass of 12.5 wt%, which is significantly higher than the theoretical residual content (10.7 wt%) and that of ABS3. These findings demonstrate that the introduction of cerium enhances the thermal condensation of the ABS/APP/DP system at high temperatures, facilitating the formation of a stable carbon layer and improving flame-retardant performance.

3.3. Flame-retardant behaviors

As depicted in Fig. 5, pure ABS (ABS1) presented an LOI value of 19.4% with no rating of UL-94, illustrating its high flammability. The incorporation of flame retardants improved the LOI

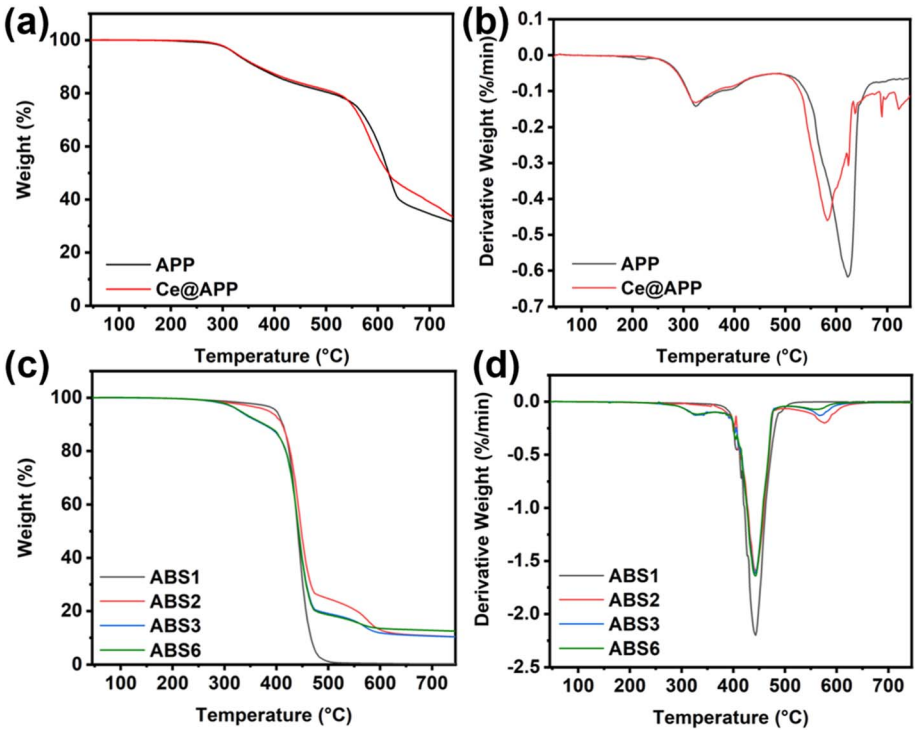

Fig. 4 TG (a) and DTG (b) curves of APP and Ce@APP. TG (c) and DTG (d) curves of ABS composites.

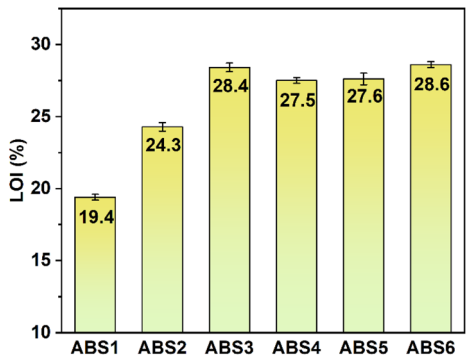

Fig. 5 LOI and UL-94 curves of ABS composites.

values of the ABS composites. Specifically, the LOI values of ABS2 and ABS3 increased to 24.3% and 28.4%, respectively, although neither achieved a V0 rating. With the introduction of Ce@APP/DP, the LOI values of the ABS composites further increased with increasing flame retardant content. Notably, ABS6 achieved an LOI value of 28.6% and successfully attained a V0 rating of UL-94, which was superior to some reported APP systems.[36,37] The phenomenon demonstrated that the Ce^{3+} enhanced the flame-retardant synergistic effect within the APP/DP system, thereby enhancing the fire safety of ABS composites.

The cone calorimeter test (CCT) results of the ABS composites are presented in Fig. 6 and Table 2. After ignition, pure ABS exhibited a sharp increase in the heat release rate (HRR), reaching a pHRR of 1132.4 kW m^{-2} at 160 s, followed by a rapid decline. This behavior was characterized by "non-carbon-forming" materials, and no residuals were observed after CCT. APP, APP/DP, and Ce@APP/DP significantly reduced the pHRR values of the resulting ABS composites. Specifically, the pHRR values for ABS2, ABS3, and ABS6 were reduced to 434.6 kW m^{-2}, 276.3 kW m^{-2}, and 264.5 kW m^{-2}, corresponding to reductions of 61.6%, 75.6%, and 76.6% compared to those of pure ABS, respectively. Additionally, the HRR curves of the flame-retardant ABS materials quickly stabilized after ignition, suggesting that the formation of the carbon layer could provide strong protection during combustion.[38] Notably, ABS3 and ABS6 exhibited lower HRR values, indicating a superior capacity to suppress heat release. In the later stages of combustion (>250 s), the HRR curve of ABS3 slightly increased, while ABS6 exhibited a sharp decrease. This phenomenon could be attributed to the instability and rupture of the carbon layers formed in ABS3, which exhibited poorer protection during the long combustion process than ABS6. In contrast, the carbon layers formed in ABS6 were more robust and stable, highlighting the superior condensed-phase effect of Ce@APP/DP. The curves matched the thermogravimetric analysis results. Therefore, the total heat release (THR) value for ABS6 was reduced to 68.3 MJ m^{-2} from 101.0 MJ m^{-2} of pure ABS, corresponding to a reduction of 32.4%. The effective heat of combustion (EHC) provides insights into the combustion behavior of volatile components in the gas phase.[39] Lower EHC values indicate incomplete combustion in the gas phase and a stronger gas-phase flame-retardant mechanism. As depicted in Table 2, the average effective heat of combustion (Av-EHC) values for all flame-retardant ABS composites were lower than those of pure ABS composites, demonstrating the presence of gas-phase flame-

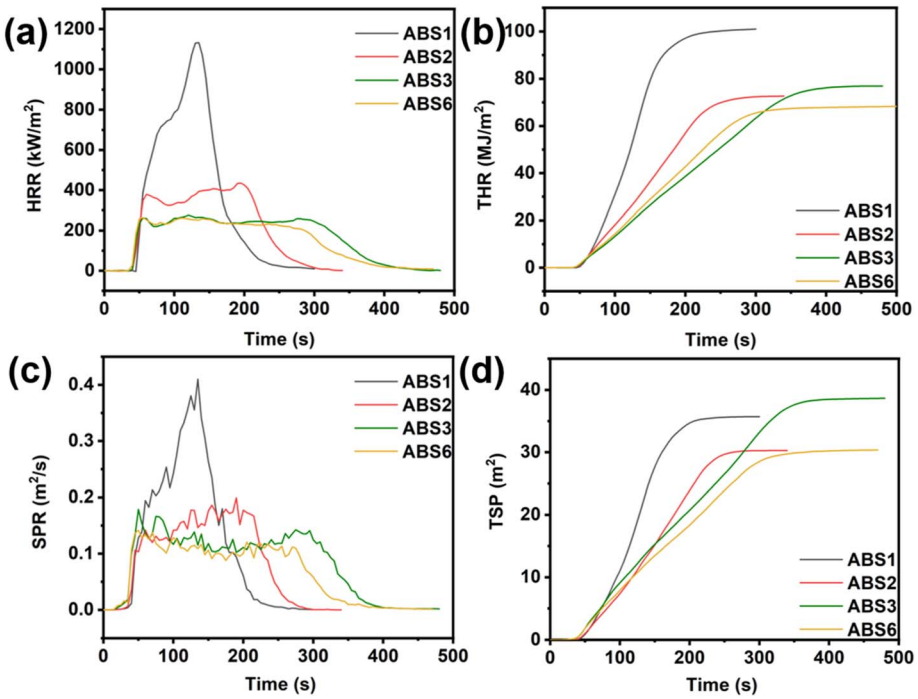

Fig. 6 Heat release rate (a), total heat release (b), smoke production rate (c), and total smoke production (d) curves of ABS composites.

Table 2 Cone calorimeter data of ABS composites

Sample	ABS1	ABS2	ABS3	ABS6
TTI (s)	40	36	35	34
PHRR (kW m^{-2})	1132.4	434.6	276.3	264.5
THR (MJ m^{-2})	101.0	72.6	77.0	68.3
Av-EHC (MJ kg^{-1})	30.3	24.6	22.8	22.7
SPR (m^2 s^{-1})	0.41	0.20	0.18	0.14
TSP (m^2)	35.7	30.3	38.6	30.4
Residue (%)	0.03	24.9	20.7	21.0

retardant effects in all three systems. Among them, APP/DP and Ce@APP/DP exhibited the lowest Av-EHC values, suggesting that the introduction of DP enhanced the gas-phase flame-retardant effects in ABS composites. These findings are consistent with the gas-phase dominant flame-retardant mechanism of DP.

The combustion of polymer materials is often accompanied by substantial smoke release, which negatively pollutes the environment and hampers the evacuation of individuals during fire.[40] In particular, heavy smoke is released in the ABS combustion. Therefore, the evaluation of smoke release is a crucial aspect of assessing the fire safety of ABS.[41] As illustrated in Fig. 6c and d, the pSPR and total smoke production (TSP) of pure ABS resin were 0.41 m^2 s^{-1} and 35.7 m^2, respectively. For ABS2, the smoke release was reduced because APP could convert volatile pyrolysis products into solid-phase residuals. Owing to the strong gas-phase effect of DP, the combustion of ABS3 turned into incomplete combustion; thus, it also destroyed the thermal stability of the carbon layers, leading to the generation of more smoke. Notably, the ABS6 demonstrated the lowest smoke release among them, where its pSPR and TSP values reduced to 0.14 m^2 s^{-1} and 30.4 m^2, respectively, decreasing by 65.9% and 14.8% compared to pure ABS. The enhanced smoke suppression of ABS6 could be attributed to the presence of Ce ions. Ce ions catalyzed the rapid formation of the dense and stable carbon layers during the combustion of the APP/DP/ABS system, improving the carbon layer's thermal stability and reducing the heat release of ABS.[42] Meanwhile, Ce ions promoted the conversion of combustible components in ABS and DP into solid residues, thereby reducing smoke generation. The synergistic flame-retardant effect of Ce@APP and DP enabled an effective balance between gas-phase and condensed-phase flame-retardant mechanisms, significantly improving the heat release and smoke suppression of ABS composites.

3.4. Flame-retardant mechanism of ABS composites

Digital photographs of the residues obtained after the cone calorimetry test of the ABS composites are presented in Fig. 7. The residues of ABS1 were minimal, further confirming that ABS was a "non-carbon-forming" material with significant heat release, resulting in severe damage to the aluminum foil. In the cases of ABS2 and ABS3, the residues exhibited a structure of complete and non-intumescent carbon layers. In contrast, the residues of ABS6 showed complete and intumescent carbon layers. Generally, the complete and intumescent carbon layers could slow down the transfer of heat and oxygen between the gas phase and the condensed phase, providing an excellent "physical barrier" effect, which could function effectively in protecting the ABS substrate during combustion, thereby enhancing its fire safety.

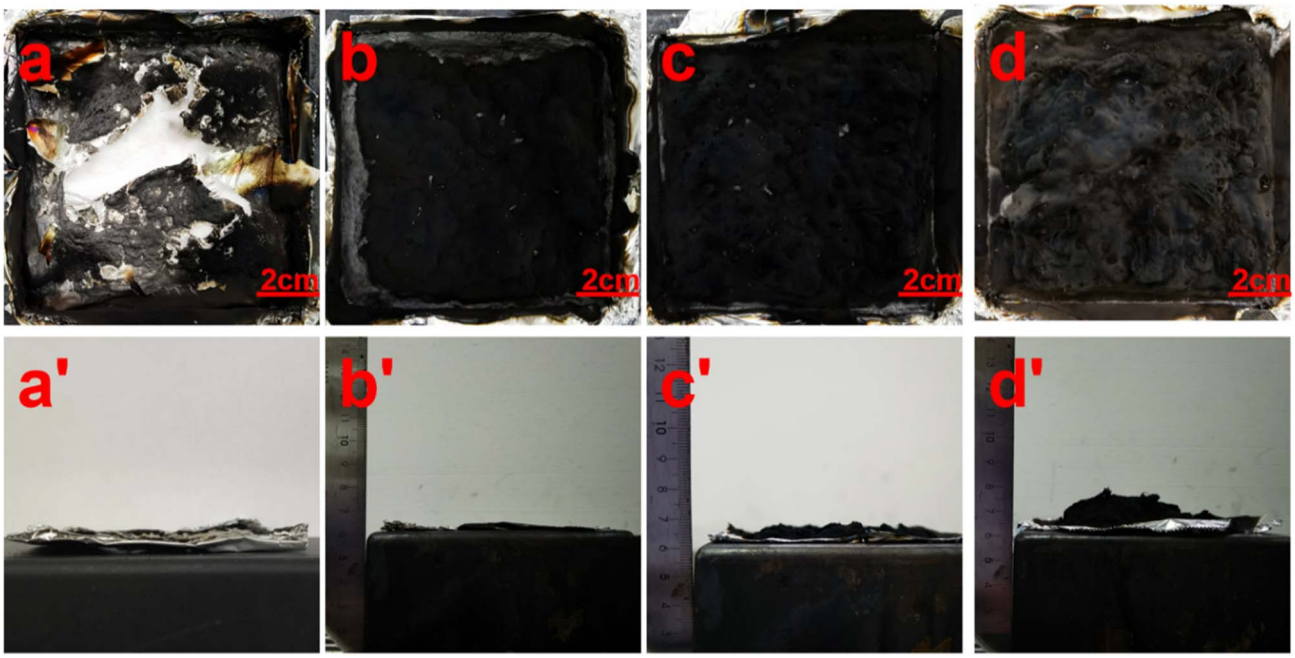

Fig. 7 Top and front views of char residues of ABS1 (a and a′), ABS2 (b and b′), ABS3 (c and c′) and ABS6 (d and d′) after the CC test.

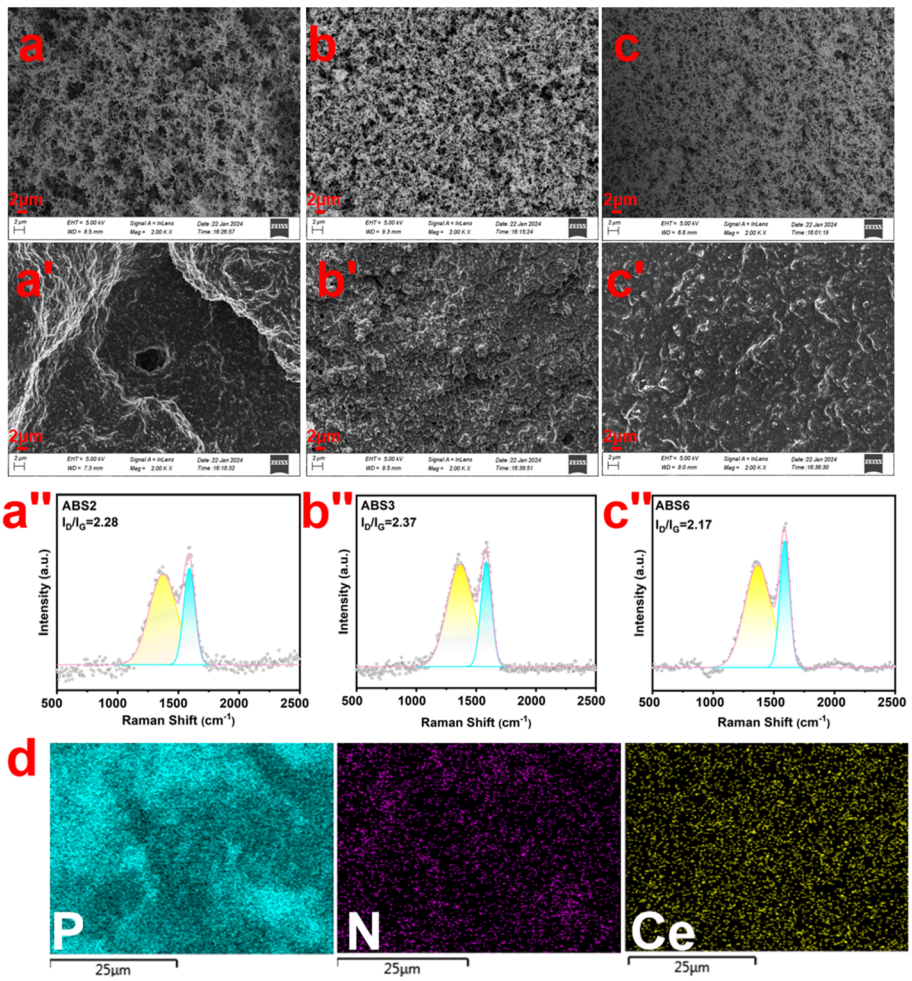

Fig. 8 SEM images and Raman spectra of char residues of ABS2 (a–a″), ABS3 (b–b″), and ABS6 (c–c″) after the cone calorimeter test. Corresponding elemental mappings of char residues of ABS6 (d).

SEM and Raman spectroscopy were employed to analyze the microstructure of the carbon layers after CCT. As depicted in Fig. 8, compared to ABS2 and ABS3, the inner and outer surfaces of the ABS6 residues exhibited a denser and more complete microstructure following the incorporation of Ce@APP/DP. Additionally, Raman spectroscopy was used to further characterize the microstructure of the residues. Typically, a lower I_D/I_G ratio indicates a higher degree of graphitization and denser residue structures.[43] The calculated I_D/I_G ratios for ABS2, ABS3, and ABS6 are 2.28, 2.37, and 2.17, respectively. Here, the residue structures of ABS2 are mainly contributed by the catalytic carbonization of APP. For ABS3, although the introduction of DP can enhance the gas-phase flame retardant effect, excessive gas-phase action damages the microstructure of carbon layers formed by ABS/APP composite, so the calculated I_D/I_G ratios for ABS3 are higher than that of ABS2. The lowest ratio of ABS6 indicates that the residues of ABS6 after the cone calorimeter test possessed the highest degree of graphitization and densest residue structures. Energy-dispersive X-ray spectroscopy analysis confirmed that phosphorus and cerium elements were uniformly distributed across the residues of ABS6. These findings indicated that the Ce@APP/DP possessed a better synergistic catalytic charring formation with DP, which could promote the formation of carbon residues and enhance the

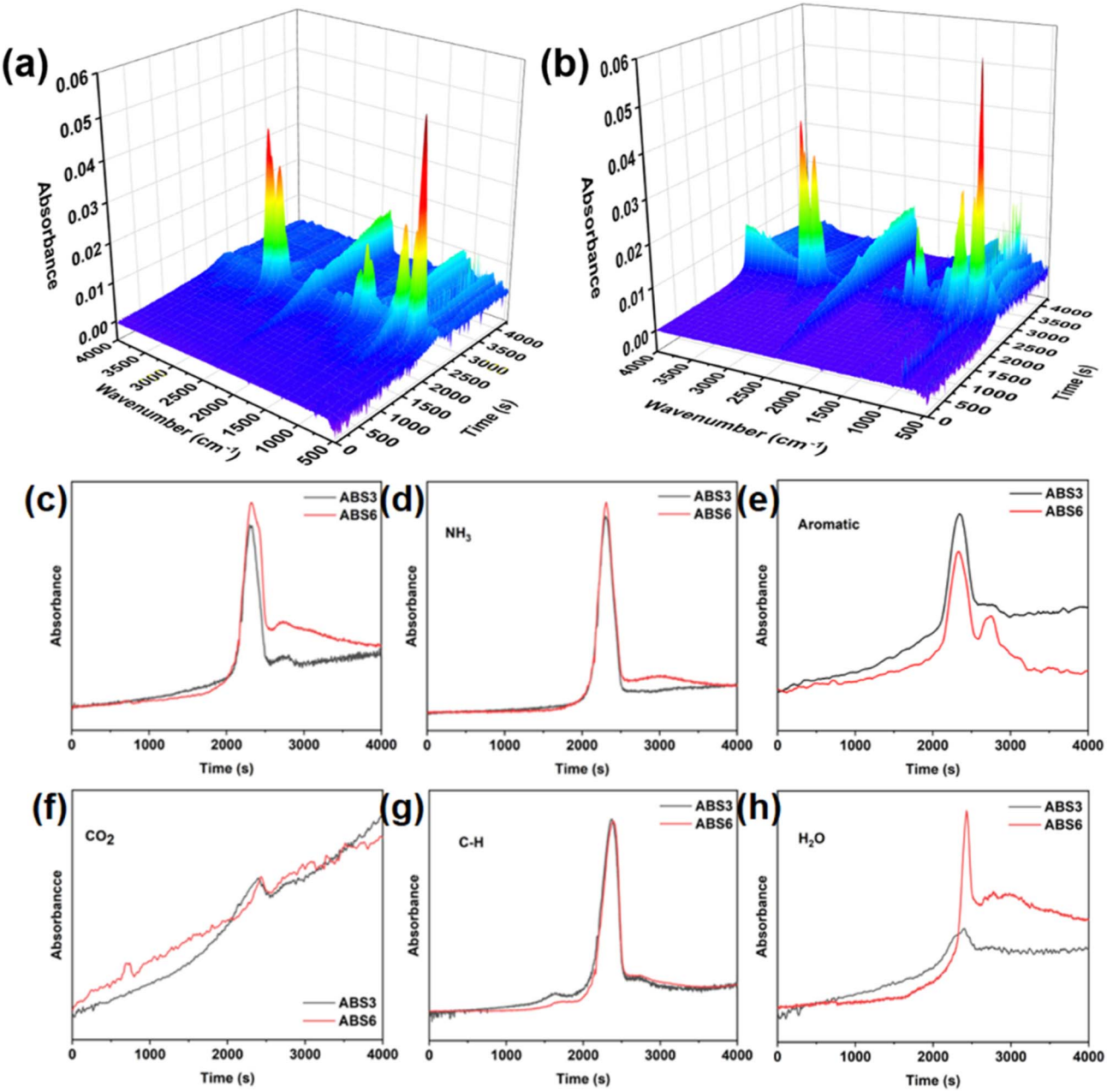

Fig. 9 3D Fourier infrared spectrum spectra of ABS3 (a) and ABS6 (b). FTIR spectra of the total gaseous products (c). Absorption intensities of pyrolysis gases of ABS3 and ABS6 (d–h).

cross-linking reactions within the carbon layers at elevated temperatures, thus forming satisfactory micro-graphitized structures. Consequently, the continuous, dense, and stable intumescent carbon layers provided robust protection to the ABS substrate during combustion and significantly improved its fire safety.

To further investigate the flame-retardant mechanism of Ce@APP/DP in ABS, thermogravimetric analysis coupled with Fourier transform infrared spectroscopy (TG-FTIR) was utilized to study the structural information of gas-phase volatile products during thermal decomposition. The 3D infrared spectra (Fig. 9a and b) demonstrated that the gas-phase volatile products of ABS3 and ABS6 were qualitatively similar, respectively. However, significant differences were observed in the appearance time and contents of volatile products released. Throughout the entire thermal decomposition process, the primary pyrolysis volatiles were identified at characteristic wavenumbers: 3500–3900 cm^{-1} (H_2O), 2700–3000 cm^{-1} (C–H), 2356 cm^{-1} (CO_2), 1560 cm^{-1} (aromatic compounds), and 930–965 cm^{-1} (NH_3).[44,45] As shown in Fig. 9c, the total release of gas-phase products for ABS3 and ABS6 was similar before 2500 s. However, after 2500 s, ABS6 exhibited a clearly higher release of gas-phase products compared to ABS3. This indicated a change in the thermal decomposition behavior of ABS6 at elevated temperatures, which was consistent with the heat release and smoke release trends observed in the TGA and CCT results. Fig. 9d–h illustrates the release profiles of specific gas-phase products. The release contents of H_2O and NH_3 for ABS3 and ABS6 were also similar prior to 2500 s, but ABS6 showed a marked increase in gas-phase product release after 2500 s, which primarily originated from the generation of pyrophosphate derivatives of APP.[46,47] These phenomena suggested that the introduction of cerium facilitated the acceleration and enhancement of APP pyrophosphorylation, promoting the formation of dense and stable high-temperature carbon layers,[48] which was critical for improving the flame retardancy of ABS6. In comparison to ABS3, ABS6 exhibited a higher release of CO_2, while the concentrations of C–H and other derivative gas-phase products remained similar. The increased release of nonflammable gases, such as H_2O, NH_3, and CO_2 reduced the concentration of combustible gases, thereby effectively limiting the combustion of ABS. Concurrently, DP and APP contributed to capturing combustible free radicals through the generation of phosphorus-containing derivatives at elevated temperatures, further decreasing the concentration of combustible gases. Additionally, the release of benzene derivatives in ABS6 was consistently low, suggesting that ABS6 produced less smoke during combustion, which also helped reduce the release of toxic gases. These results highlighted that Ce could alter the decomposition mode of the ABS/APP/DP system at high temperatures, enhancing the release of nonflammable gases and diminishing the emission of benzene derivatives and smoke toxicity.

Based on the combined analysis of TG, gas-phase, and solid-phase data, the proposed flame-retardant mechanism of Ce@APP/DP in ABS is shown in Fig. 10. Below 570 °C, the flame-retardant mechanisms of APP/DP and Ce@APP/DP systems in ABS were similar. Here, APP and DP released approximate amounts of nonflammable gases, such as H_2O, NH_3, CO_2, and phosphorus-benzene derivatives. These compounds could

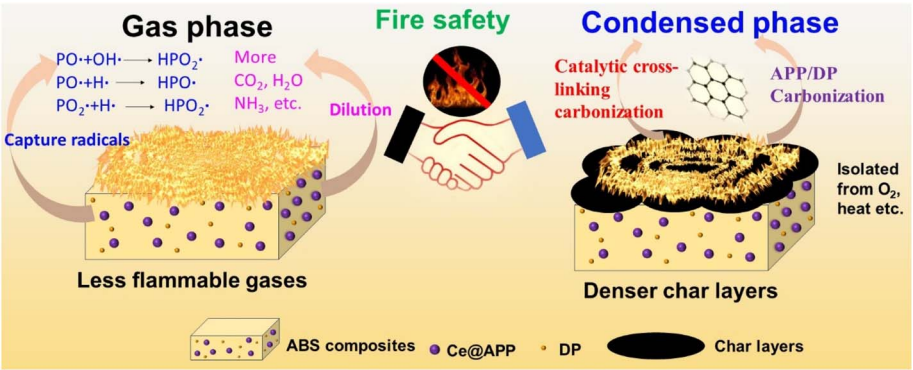

Fig. 10 Possible flame-retardant mechanism of Ce@APP/DP in ABS.

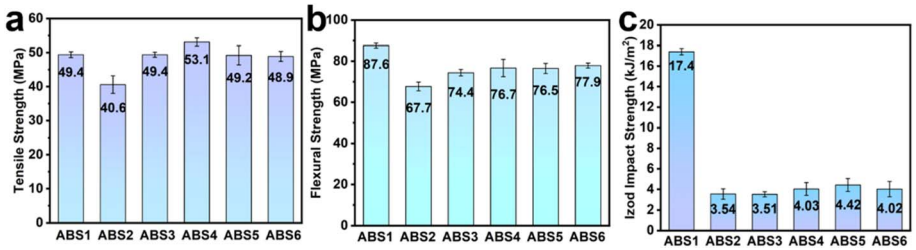

Fig. 11 Tensile strength (a), flexural strength (b) and impact strength (c) of ABS composites.

capture combustible free radicals and dilute the concentrations of combustible gases and oxygen, thus contributing to gas-phase flame retardancy. After 570 °C, the presence of Ce changed the decomposition process and residue formation. Specifically, Ce accelerated the pyrophosphorylation of APP, promoting the cross-linking reaction of the carbon layers in ABS6 at high temperatures, which resulted in the formation of a well-graphitized structure. Moreover, Ce enhanced the release of nonflammable gases, such as H_2O, NH_3, and CO_2, which combined with the phosphorus-containing derivatives generated by DP and APP, capturing combustible free radicals and further reducing the concentration of combustible gases. This process enabled the formation of continuous, dense, and stable intumescent carbon layers that protected the ABS substrates during combustion, thereby improving fire safety.

3.5 Mechanical properties of ABS composites

The mechanical properties of the ABS composites are illustrated in Fig. 11. After the incorporation of APP, the tensile strength and flexural strength of ABS2 decreased to 82.2% and 77.3% with respect to ABS1, respectively. Meanwhile, the impact strength was only 3.54 kJ m^{-2}, suggesting poor compatibility between APP and ABS substrates.[48] In contrast, DP exhibited better interface compatibility with the ABS substrate compared to APP. Consequently, the tensile strength and flexural strength of ABS3 significantly improved, reaching 49.4 MPa and 74.4 MPa, which represented an increase by 21.7% and 9.9% compared to ABS2, respectively. When Ce@APP replaced APP, it was evident that the mechanical properties of the ABS composites gradually decreased with increasing Ce@APP/DP content. However, the tensile strength and flexural strength of ABS6 were almost equivalent to those of ABS1. Notably, ABS6 achieved an impact strength of 4.02 kJ m^{-2}, which was higher than the 3.54 kJ m^{-2} of ABS2 and 3.51 kJ m^{-2} of ABS3. Compared with previous studies,[36,37] ABS6 displayed high mechanical properties, especially impact strength. These results demonstrated that the introduction of Ce did not deteriorate the compatibility between the APP/DP system and the ABS matrix.

4 Conclusion

In this study, we successfully synthesized Ce@APP using a simple and environmentally friendly ion exchange method and then incorporated it with DP to flame retard ABS composites. When 30% Ce@APP/DP was added, the LOI of ABS6 reached 28.6% and reached the V0 level of UL-94. Notably, compared to pure ABS, the heat and smoke release of ABS6 were significantly reduced during combustion. The introduction of Ce at high temperatures (above 570 °C) altered the thermal decomposition process of the ABS/APP/DP system, which accelerated the pyrophosphorylation of APP, thereby enhancing the cross-linking reaction of the carbon layers in the ABS6 at high temperatures. Additionally, the release of noncombustible gases and the capture of combustible free radicals by phosphorus derivatives increased, fostering a strong catalytic synergistic effect. This led to the formation of compact and stable intumescent carbon layers, thereby achieving remarkable fire safety. Furthermore, the good interfacial compatibility between the Ce@APP/DP system and ABS mitigated the deterioration of the mechanical properties of the flame-retardant ABS. The tensile strength and flexural strength of ABS6 remained comparable to those of pure ABS, while the impact strength reached 4.02 kJ m^{-2}. Therefore, this study presented a method for obtaining halogen-free flame-retardant ABS composites with high fire safety and mechanical properties.

Data availability

Data will be made available on request.

Author contributions

Ping Meng: writing – original draft, resources, investigation, and formal analysis. Hong-Ren Xiao: resources, investigation, and formal analysis. Feng Zhang: resources and investigation. Rui-Sheng Jia: investigation. Longxiang Zhu: writing – review & editing. Zhu-Bao Shao: visualization, supervision, and formal analysis.

Conflicts of interest

The authors declare that they have no competing interests.

Acknowledgements

This work was supported by the Taishan Scholar Program of Shandong Province (tsqn202211126).

References

1 Y. Lin, S. Li, L. Du, W. Dong, X. Chen, Q. Gao and B. Wang, Interfacial engineering of 0D-2D hierarchical MXene@PEI@AgNC nanohybrids to achieve flame retardant, mechanical and antibacterial properties of ABS nanocomposites, *Chem. Eng. J.*, 2024, **499**, 156288.
2 P. Yaman, S. S. Karabeyoglu and A. Moralar, Investigation of mechanical and frictional properties of ulexite and colemanite filled acrylonitrile-butadiene-styrene polymer composites for industrial use, *J. Thermoplast. Compos.*, 2023, **37**(10), 3136–3157.
3 X. Hu, Y. Guo, L. Chen, X. Wang, L. Li and Y. Wang, A novel polymeric intumescent flame retardant: Synthesis, thermal degradation mechanism and application in ABS copolymer, *Polym. Degrad. Stab.*, 2012, **979**, 1772–1778.
4 Z. Yuan, H. Wen, Y. Liu and Q. Wang, Synergy between piperazine pyrophosphate and aluminum diethylphosphinate in flame retarded acrylonitrile-butadiene-styrene copolymer, *Polym. Degrad. Stab.*, 2021, **190**, 109639.
5 B. Prieur, M. Meub, M. Wittemann, R. Klein, S. Bellayer, G. Fontaine and S. Bourbigot, Phosphorylation of lignin to

flame retard acrylonitrile butadiene styrene (ABS), *Polym. Degrad. Stab.*, 2016, **127**, 32–43.
6 H. Fu, Y. Bai, S. Q. Duan, H. F. Zhou and W. Gong, Structure design of multi-layered ABS/CNTs composite foams for EMI shielding application with low reflection and high absorption characteristics, *Appl. Surf. Sci.*, 2023, **624**, 157168.
7 C. Yildiz, Y. Seki, E. Kizilkan, M. Sarikanat and L. Altay, Development of Halogen-Free Flame Retardant Acrylonitrile Butadiene Styrene (ABS) Based Composite Materials, *ChemistrySelect*, 2023, **841**, e202300989.
8 A. Bachinger, A. Sandinge, K. M. Lindqvist, A. Strid and G. Gong, Systematic evaluation of bromine-free flame-retardant systems in acrylonitrile-butadiene-styrene, *J. Appl. Polym. Sci.*, 2021, **13913**, e51861.
9 D. Hu, Q. Zhou and K. Zhou, Combined effects of layered nanofillers and intumescent flame retardant on thermal and fire behavior of ABS resin, *J. Appl. Polym. Sci.*, 2019, **13646**, 48220.
10 Y. Yang, H. Luo, X. Cao, F. Zhou, W. Kong and X. Cai, The synergistic effects of a novel intumescent flame-retardant poly-(4-nitrophenoxy)-phosphazene and ammonium polyphosphate on ABS systems, *J. Therm. Anal. Calorim.*, 2018, **1371**, 65–77.
11 N. Wu, Z. Xiu and J. Du, Preparation of microencapsulated aluminum hypophosphite and flame retardancy and mechanical properties of flame-retardant ABS composites, *J. Appl. Polym. Sci.*, 2017, **13433**, 45008.
12 Y. Xia, X. Jian, J. Li, X. Wang and Y. Xu, Synergistic Effect of Montmorillonite and Intumescent Flame Retardant on Flame Retardance Enhancement of ABS, *Polym. Plast. Technol. Eng.*, 2007, **463**, 227–232.
13 R. Jian, L. Chen, B. Zhao, Y. Yan, X. Li and Y. Wang, Acrylonitrile-butadiene-styrene terpolymer with metal hypophosphites: flame retardance and mechanism research, *Ind. Eng. Chem. Res.*, 2014, **53**, 2297–2307.
14 Y. Lin, W. Dong, S. Li, S. Zhang, X. Chen, L. Du and B. Wang, Core-shell Ag@PZS modified MXene towards highly flame retardancy, electromagnetic interference shielding, antibacterial of robust tough hierarchical ABS composites, *Composites, Part A*, 2025, **192**, 108726.
15 V. Realinho, D. Arencón, M. Antunes and J. I. Velasco, Effects of a Phosphorus Flame Retardant System on the Mechanical and Fire Behavior of Microcellular ABS, *Polymers*, 2018, **111**, 30.
16 R. Jian, L. Chen, S. Chen, J. Long and Y. Wang, A novel flame-retardant acrylonitrile-butadiene-styrene system based on aluminum isobutylphosphinate and red phosphorus: Flame retardance, thermal degradation and pyrolysis behavior, *Polym. Degrad. Stab.*, 2014, **109**, 184–193.
17 R. Jian, L. Chen, Z. Hu and Y. Wang, Flame-retardant polycarbonate/acrylonitrile-butadiene-styrene based on encapsulated red phosphorus by polysiloxane: flame retardancy, thermal stability and water resistance, *J. Appl. Polym. Sci.*, 2012, **123**, 2867–2874.
18 H. Mo, L. Xu and T. Zhou, Novel synergistic flame-retardant system of Mg–Al–Co–LDHs/DPCPB for ABS resins, *J. Appl. Polym. Sci.*, 2018, **13522**, 46319.
19 D. Hwang, S. G. Lee and D. Cho, Dual-Sizing Effects of Carbon Fiber on the Thermal, Mechanical, and Impact Properties of Carbon Fiber/ABS Composites, *Polymers*, 2021, **1314**, 2298.
20 Z. Shao, C. Deng, Y. Tan, M. Chen, L. Chen and Y. Wang, An Efficient Mono-Component Polymeric Intumescent Flame Retardant for Polypropylene: Preparation and Application, *ACS Appl. Mater. Interfaces*, 2014, **610**, 7363–7370.
21 P. Li, H. Liu, Y. Xu, D. Wang, Y. Liu and P. Zhu, Flame-retardant and antibacterial flexible polyurethane foams with high resilience based on a P/N/Si-containing system, *J. Mater. Sci. Technol.*, 2024, **182**, 141–151.
22 S. Chen, Z. Chen, W. Bi, W. Du, L. Lin, D. Hu and H. Zhuo, Development of a Zr-Based Metal–Organic Framework (UiO-66) for a Cooperative Flame Retardant in the PC/ABS, *Polymers*, 2024, **16**, 2083.
23 H. Ma, L. Tong, Z. Xu, Z. Fang, Y. Jin and F. Lu, A novel intumescent flame retardant: Synthesis and application in ABS copolymer, *Polym. Degrad. Stab.*, 2007, **92**, 720–726.
24 N. Hong, J. Zhan, X. Wang, A. A. Stec, T. Richard Hull, H. Ge, W. Xing, L. Song and Y. Hu, Enhanced mechanical, thermal and flame retardant properties by combining graphene nanosheets and metal hydroxide nanorods for Acrylonitrile–Butadiene–Styrene copolymer composite, *Composites, Part A*, 2014, **64**, 203–210.
25 B. Liu, Y. Zhang, C. Wan, Y. Zhang, R. Li and G. Liu, Thermal stability, flame retardancy and rheological behavior of ABS filled with magnesium hydroxide sulfate hydrate whisker, *Polym. Bull.*, 2007, **58**, 747–755.
26 A. Rodriguez, M. Herrero, M. Asensio, M. Santiago-Calvo, J. Guerrero, E. Cañibano, M. T. Fernández and K. Nuñez, Cooperative Effect of Chemical and Physical Processes for Flame Retardant Additives in Recycled ABS, *Polymers*, 2023, **15**, 2431.
27 P. Müller and B. Schartel, Melamine poly(metal phosphates) as flame retardant in epoxy resin: Performance, modes of action, and synergy, *J. Appl. Polym. Sci.*, 2016, **13324**, 43549.
28 Z. Shao, J. Cui, X. Li, J. L. Díaz Palencia and D. Wang, Chemically inorganic modified ammonium polyphosphate as eco-friendly flame retardant and its high fire safety for epoxy resin, *Compos. Commun.*, 2021, **28**, 100959.
29 K. S. Lim, S. T. Bee, L. T. Sin, T. T. Tee, C. T. Ratnam, D. Hui and A. R. Rahmat, A review of application of ammonium polyphosphate as intumescent flame retardant in thermoplastic composites, *Composites, Part B*, 2016, **84**, 155–174.
30 Z. Shao, J. Zhang, R. Jian, C. Sun, X. Li and Y. Wang, A strategy to construct multifunctional ammonium polyphosphate for epoxy resin with simultaneously high fire safety and mechanical properties, *Composites, Part A*, 2021, **149**, 106529.
31 Z. Shao, J. Cui, X. Lin, X. Li, R. Jian and Y. Wang, In-situ coprecipitation formed Fe/Zn-layered double hydroxide/ammonium polyphosphate hybrid material for flame retardant epoxy resin via synergistic catalytic charring, *Composites, Part A*, 2022, **155**, 106841.

32 Z. Shao, M. Zhang, Y. Han, X. Yang, J. Jin and R. Jian, A highly efficient gas-dominated and water-resistant flame retardant for non-charring polypropylene, *RSC Adv.*, 2017, **782**, 51919–51927.

33 X. Song, H. Lv, M. Shi, Z. Shao and Y. Wang, Calcium gluconate-based flame retardant towards simultaneously high-efficiency fire safety and mechanical enhancement for epoxy resin, *Int. J. Biol. Macromol.*, 2024, **264**, 130409.

34 S. Bee, K. Lim, L. T. Sin, C. T. Ratnam, S. L. Bee and A. R. Rahmat, Interactive effect of ammonium polyphosphate and montmorillonite on enhancing flame retardancy of polycarbonate/acrylonitrile butadiene styrene composites, *Iran. Polym. J.*, 2018, **2711**, 899–911.

35 M. Wan, C. Shi, X. Qian, Y. Qin, J. Jing, H. Che, F. Ren, J. Li, B. Yu and K. Zhou, Design of novel double-layer coated ammonium polyphosphate and its application in flame retardant thermoplastic polyurethanes, *Chem. Eng. J.*, 2023, **459**, 141448.

36 X. Cao, Y. Yang, H. Luo and X. Cai, High efficiency intumescent flame retardancy between Hexakis (4-nitrophenoxy) cyclotriphosphazene and ammonium polyphosphate on ABS, *Polym. Degrad. Stab.*, 2017, **143**, 259–265.

37 N. Wu, Z. Xiu and J. Du, Preparation of microencapsulated aluminum hypophosphite and flame retardancy and mechanical properties of flame-retardant ABS composites, *J. Appl. Polym. Sci.*, 2017, **134**, 45008.

38 G. Huang, S. Huo, X. Xu, W. Chen, Y. Jin, R. Li, P. Song and H. Wang, Realizing simultaneous improvements in mechanical strength, flame retardancy and smoke suppression of ABS nanocomposites from multifunctional graphene, *Composites, Part B*, 2019, **177**, 107377.

39 F. Zhou, W. Tang, W. Xi, L. Qian, J. Wang, Y. Qiu and Y. Chen, Improving the fracture toughness, flame retardancy and smoke suppression of ABS by core-shell elastic flame retardant particles with P/Si synergistic effect, *Polym. Degrad. Stab.*, 2024, **228**, 110893.

40 Y. Shi, B. Yu, X. Wang and A. C. Y. Yuen, Editorial: Flame-Retardant Polymeric Materials and Polymer Composites, *Front. Mater.*, 2021, **8**, 703123.

41 J. Yi, Y. Liu and X. Cai, The synergistic effect of adjuvant on the intumescent flame-retardant ABS with a novel charring agent, *J. Therm. Anal. Calorim.*, 2012, **1132**, 753–761.

42 X. Li, F. Zhang, M. Zhang, X. Zhou and H. Zhang, Comparative Study on the Flame Retardancy and Retarding Mechanism of Rare Earth (La, Ce, and Y)-Based Organic Frameworks on Epoxy Resin, *ACS Omega*, 2021, **651**, 35548–35558.

43 B. Wang, L. Zhang, W. Song and Y. Liu, Alkaline amino acid modification based on biological phytic acid for preparing flame-retardant and antibacterial cellulose-based fabrics, *Int. J. Biol. Macromol.*, 2024, **276**, 134002.

44 J. Feng, C. Carpanese and A. Fina, Thermal decomposition investigation of ABS containing Lewis-acid type metal salts, *Polym. Degrad. Stab.*, 2016, **129**, 319–327.

45 Z. Yang, Z. Gu, X. Yang, Z. Zhang, X. Wang, X. Chen and L. Yang, The mechanism study on the cooperative flame resistance effect between HMP and NP in ABS by TG–FTIR, *J. Therm. Anal. Calorim.*, 2017, **1291**, 303–314.

46 W. Jun, L. Yi and X. Cai, Effect of a novel charring agent on thermal degradation and flame retardancy of acrylonitrile–butadiene–styrene, *J. Therm. Anal. Calorim.*, 2010, **1032**, 767–772.

47 X. Ye, Y. Wang, Z. Zhao and H. Yan, A novel hyperbranched poly(phosphorodiamidate) with high expansion degree and carbonization efficiency used for improving flame retardancy of APP/PP composites, *Polym. Degrad. Stab.*, 2017, **142**, 29–41.

48 X. Bi, K. Song, Q. Li, T. Lin, Y. Pan, W. Wang, J. He and R. Yang, Restriction of Ce-MOF growth within ZSM zeolite for robust three-proofing thermoplastic polyurethane, *J. Mater. Chem. A*, 2024, **1246**, 32030–32044.